Coherent Nonlinear Coupling between a Long-Wavelength Mode and Small-Scale Turbulence in the TEXT Tokamak

H. Y. W. Tsui, K. Rypdal,[a] Ch. P. Ritz, and A. J. Wootton
Fusion Research Center, The University of Texas at Austin, Austin, Texas 78712
(Received 4 November 1992)

Bispectral analysis of Langmuir probe data indicates that coherent nonlinear coupling, in addition to the noncoherent turbulent interactions, exists in the edge plasma of the tokamak TEXT. Not all the modes involved reside within the spectral region of the usual broadband turbulence. At a major resonant surface the small-scale turbulent activity interacts *coherently* with a localized long-wavelength mode; a signature of regular or coherent structure. By the observed coupling to the transport related turbulence, the long-wavelength mode can influence plasma confinement indirectly. These observations signify the influence of low-order resonant surfaces on the edge turbulence in tokamaks.

PACS numbers: 52.35.Mw, 52.35.Ra, 52.55.Fa

Turbulence is thought to be important in determining the transport of energy and particles in toroidally confined plasmas of fusion interest [1]. In addition to being accessible to probing, the edge region of these plasmas has been studied extensively because of its overall relationship to confinement. Experiments to date show that interactions and couplings between spontaneously excited fluctuations can lead to turbulence-induced particles and energy fluxes that dominate the transport in the edge of tokamaks ([2] and references therein) as well as in the edge of other magnetically confined toroidal plasmas (e.g., [3]). Thus, it is important to understand and to control the turbulence-induced transport. The edge turbulence in tokamaks has been associated with a number of driving mechanisms, although it has been widely assumed that the turbulence is the nonlinear stage of linearly unstable modes of drift type (e.g., [4]). Theoretical studies of turbulence often predict that inverse cascade leads to large-scale vortexlike structures coexisting with the small-scale turbulence [5–9]. Nonlinear interactions between the long-wavelength and the short-wavelength modes can significantly affect the dynamics of the system such as self-organization and the formation of regular structure.

In the Texas Experimental Tokamak (TEXT) the edge turbulence (at $r \lesssim a$) is typically distributed in a broad frequency band 50–150 kHz [10], although isolated spectral peaks often exist in the power spectra obtained from fluctuation measurements near major resonant surfaces. For instance, near the magnetic flux surface having a safety factor $q = rB_\phi/RB_\theta = 3$, a feature with properties different from those of the broadband turbulence has been observed at a frequency of 20 kHz [11]. Examples of the power spectra obtained from Langmuir probe measurements of floating potential fluctuations ($\tilde{\varphi}$) at the $q = 3$ (solid line) and at $q = 3.1$ (dotted line) flux surfaces are reproduced here in Fig. 1(a). There is a low-frequency "quasicoherent" mode, so named because of its relatively narrow spectral peak, confined to the $q = 3$ flux surface. The (half) radial mode width was estimated to be less than 3 mm. Using a two-point correlation technique [12], it was determined that the 20 kHz quasicoherent mode has relatively long wavelength ($\bar{k}_\theta \approx 50\ \mathrm{m}^{-1}$ or poloidal mode number $m = 12$) compared to those of the broadband turbulence ($\bar{k}_\theta = 300\ \mathrm{m}^{-1}$ or $m = 75$ at the broadband spectral peak of 100 kHz). It propagates in the same (electron diamagnetic drift) direction as the broadband modes and has relatively faster phase velocity. In terms of the collisionality parameter $k_\parallel^2 v_{\mathrm{th}}^2/\omega\nu_e$ [13], the low-frequency mode is collisional and the broadband

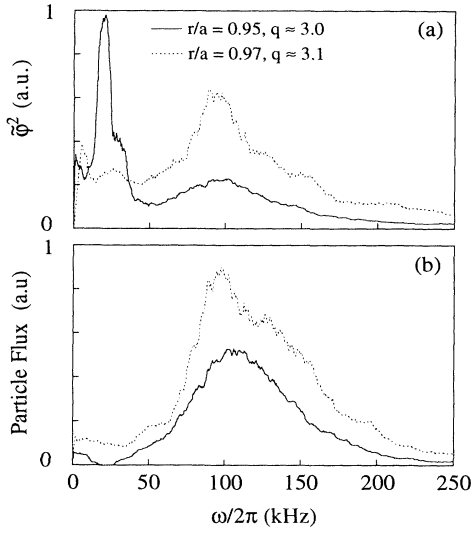

FIG. 1. (a) Power spectra of the Langmuir probe floating potential fluctuations ($\tilde{\varphi}$) and (b) spectra of the electrostatic fluctuation-driven particle flux, obtained from a cross correlation between the density fluctuations $\tilde{n}$ and the poloidal electric field fluctuations $\tilde{E}_\theta$, at $r/a = 0.95$ (solid line) and $r/a = 0.97$ (dotted line). At $r/a = 0.95$, corresponding to the $q = 3$ flux surface, a peak at $\omega/2\pi = 20$ kHz coexists with the broadband activities centered at $\omega/2\pi \approx 100$ kHz. In spite of its large amplitude, the low-frequency activity does not contribute much to the particle flux.

turbulence is semicollisional. These results are consistent with predictions based on kinetic theory of tearing modes [14,15] or the drift-resistive MHD theory for drift-tearing modes [16] and drift-ripping modes [17]. In contrast to the small-scale broadband activity this mode does not contribute directly to the electrostatic fluctuation-driven particle flux [see Fig. 1(b)] though it may contribute indirectly through nonlinear interaction with the broadband turbulence. This nonlinear coupling path is the subject of the present work.

In this Letter, we describe new phenomena related to these localized quasicoherent modes. Using a bispectral analysis technique [18], we identified *coherent* nonlinear coupling between the localized long-wavelength mode and the short-wavelength modes in a frequency band in the lower part of the usual broadband spectrum. Such coupling supports the hypothesis that the quasicoherent mode can influence the small-scale turbulence and hence indirectly the associated transport. Furthermore, the analysis reveals that $\sum\gamma^2(\omega_1,\omega_2)=1$ for interactions involving the localized low-frequency mode, where γ is the bicoherence corresponding to a triplet ω_1, ω_2, and $\omega=\omega_1+\omega_2$ and the sum is over all ω_1 and ω_2 satisfying this resonance condition. This result indicates that the nonlinear interactions comprising the quasicoherent mode are coherent in contrast to the conventional picture of noncoherent strong turbulent interactions among the shorter-wavelength broadband modes. By coherent we mean that spectral broadening or phase randomization in the nonlinear process is small. In the absence of turbulent broadening, the interacting modes can stay together to form a regular or coherent structure.

Figure 2 is a three-dimensional plot of the squared bicoherence, $\gamma^2(\omega_1,\omega_2)$, computed from the same floating potential fluctuation data which has the power spectrum shown as the solid line in Fig. 1(a). The squared autobicoherence from a single spatial-point measurement which is defined as

$$\gamma^2(\omega_1,\omega_2)=\frac{|\langle\tilde{\varphi}(\omega_1)\tilde{\varphi}(\omega_2)\tilde{\varphi}^*(\omega_1+\omega_2)\rangle|^2}{\langle|\tilde{\varphi}(\omega_1)\tilde{\varphi}(\omega_2)|^2\rangle\langle|\tilde{\varphi}(\omega_1+\omega_2)|^2\rangle} \quad (1)$$

with $\langle\cdots\rangle$ denoting the ensemble average and $\tilde{\varphi}^*$ the complex conjugate of $\tilde{\varphi}$, describes the coupling among a triplet of modes at frequencies ω_1, ω_2, and $\omega=\omega_1+\omega_2$. When modes of different frequencies vary independently as in random noise the bicoherence has a value of zero. Because of the symmetry property of bicoherence, it is customary to plot the autobicoherence within the triangle $0\le\omega_2\le\omega_{NQ}/2$ and $\omega_2\le\omega_1\le\omega_{NQ}-\omega_2$ [18] where ω_{NQ} is the Nyquist frequency. The prominent peak (at $\omega_2/2\pi=20$ kHz and 20 kHz $\le\omega_1/2\pi\le 80$ kHz) in Fig. 2 indicates a significant level of nonlinear interactions concentrated at these frequencies. In this compact representation, the interactions involving the quasicoherent mode at 20 kHz are represented by $\gamma^2(\omega_1,\omega_2)$ lying on three separate straight lines: (i) $(\omega_1+\omega_2)/2\pi=20$ kHz,

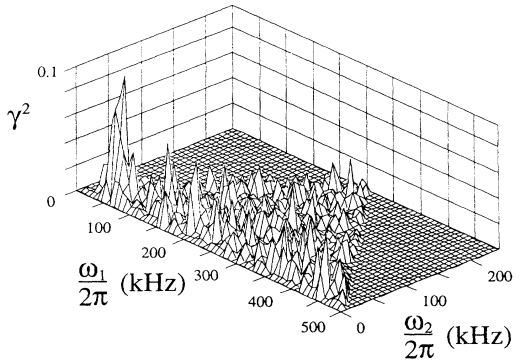

FIG. 2. The squared bicoherence $\gamma^2(\omega_1,\omega_2)$ showing three-wave interaction of modes with frequencies ω_1, ω_2, and $\omega=\omega_1+\omega_2$. There is a prominent peak at $\omega_2/2\pi=20$ kHz and 20 kHz $\le\omega_1/2\pi\le 80$ kHz.

(ii) $\omega_2/2\pi=20$ kHz, and (iii) $\omega_1/2\pi=20$ kHz inside the triangular region. The peak value of $\gamma^2\approx 0.1$ is large compared to the statistical uncertainty of 0.004 ($\approx 1/M$ where $M=240$ is the number of realizations). Values of γ^2 at other frequencies (e.g., those falling within the usual broadband activity), though less than the peak value, are still larger than the statistical uncertainties. This means that nonlinear interactions are also present among the broadband activity; a result consistent with previous studies on the coupling coefficients and power transfer functions [19]. To focus the discussion on wave-wave coupling involving the quasicoherent mode, we plot γ^2 for these interactions in Fig. 3. Here the x axis corresponds to the frequency $(\omega_1/2\pi)$ of one component of the triplet which satisfies the resonant condition $\omega_1+\omega_2=\omega_3$ with $\omega_3/2\pi$ fixed at 20 kHz. This figure shows that strong nonlinear coupling occurs between the quasicoherent mode at $\omega/2\pi=20$ kHz and frequency pairs ω_1 and

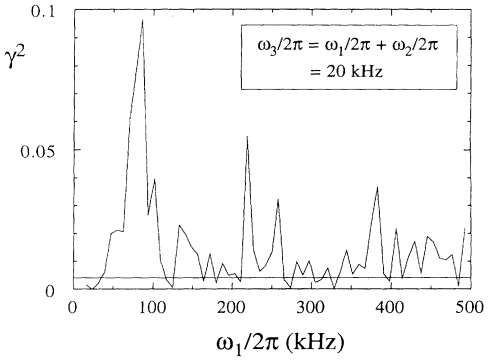

FIG. 3. The squared bicoherence $\gamma^2(\omega_1,\omega_2)$ for interactions satisfying the resonant condition $\omega_3=\omega_1+\omega_2$ with $\omega_3/2\pi$ fixed at 20 kHz. Strong nonlinear interactions occur between the quasicoherent mode at 20 kHz and modes in the frequency band of 40–100 kHz. The straight line denotes the statistical uncertainty of 0.004 in γ^2.

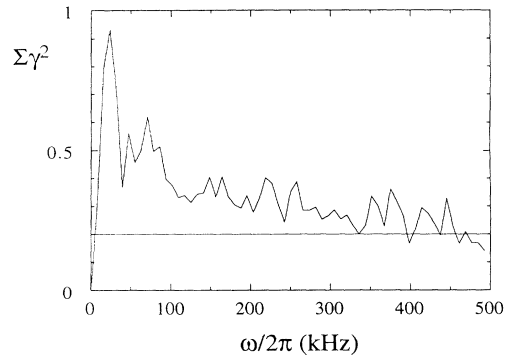

FIG. 4. The sum of squared bicoherence of the interactions involving a mode at frequency $\omega/2\pi$. At the quasicoherent mode frequency (20 kHz), the sum is close to unity. The unity sum is an indication of coherent nonlinear interaction. The straight line represents the statistical uncertainty of 0.2 in $\sum\gamma^2$.

$\omega_1+\omega_2$ in the band between 40 and 100 kHz. It is worth emphasizing that the lower frequency (and lower $\bar{k}_\theta$) components of the broadband activity dominate these nonlinear interactions.

An interesting property of the interactions connected with the quasicoherent mode is that the total squared bicoherence $\sum\gamma^2(\omega_1,\omega_2)\approx 1$. This result is shown in Fig. 4 together with the total squared bicoherence at other mode frequencies. Each value of the total squared bicoherence is a sum of γ^2 for all ω_1 and ω_2 satisfying the resonant condition $\omega=\omega_1+\omega_2$ within the reduced triangular spectral region. Only at the quasicoherent mode frequency (20 kHz) is the total squared bicoherence close to unity. Within the framework of quadratic coupling models, the unity total bicoherence indicates coherent wave coupling. The coherent wave coupling itself is indicative of regular (or coherent) structure. The less than unity total squared bicoherence at other mode frequencies (e.g., those of the broadband activity) is consistent with noncoherent turbulent interactions among the short-wavelength modes.

To prove the above conclusions, we examine the behavior of the bicoherence of a system described by a general nonlinear wave-coupling equation (an example is the Hasegawa-Mima equation [20]),

$$\frac{\partial\tilde{\varphi}_{\mathbf{k}}(t)}{\partial t}+L_{\mathbf{k}}\tilde{\varphi}_{\mathbf{k}}(t)=\sum_{\mathbf{k}'}A_{\mathbf{k},\mathbf{k}'}\tilde{\varphi}_{\mathbf{k}'}(t)\tilde{\varphi}_{\mathbf{k}-\mathbf{k}'}(t)\,, \tag{2}$$

where $L_{\mathbf{k}}$ denotes the linear and $A_{\mathbf{k},\mathbf{k}'}$ the nonlinear coupling terms. It is possible to include radial eigenmode structure using the analysis procedure of Ref. [21], although for simplicity, we proceed by ignoring the radial mode structure. In this case, we may identify $\mathbf{k}=(k_\theta,k_\phi)$. For stationary turbulence, Eq. (2) can be Fourier transformed in time to yield

$$\tilde{\varphi}_{\mathbf{k}}(\omega)=\sum_{\omega',\mathbf{k}'}\frac{A_{\mathbf{k},\mathbf{k}'}}{L_{\mathbf{k}}+i\omega}\tilde{\varphi}_{\mathbf{k}'}(\omega')\tilde{\varphi}_{\mathbf{k}-\mathbf{k}'}(\omega-\omega')\,. \tag{3}$$

In this form, the wave-coupling equation relates each $\tilde{\varphi}_{\mathbf{k}}(\omega)$ to the quadratic terms involving modes satisfying the resonant conditions in $\mathbf{k}$ and ω. Let us now examine the squared bicoherence defined in terms of the spectral components as

$$\gamma^2_{\mathbf{k},\mathbf{k}'}(\omega,\omega')=\frac{|\langle\tilde{\varphi}^*_{\mathbf{k}}(\omega)\tilde{\varphi}_{\mathbf{k}'}(\omega')\tilde{\varphi}_{\mathbf{k}-\mathbf{k}'}(\omega-\omega')\rangle|^2}{\langle|\tilde{\varphi}_{\mathbf{k}'}(\omega')\tilde{\varphi}_{\mathbf{k}-\mathbf{k}'}(\omega-\omega')|^2\rangle\langle|\tilde{\varphi}_{\mathbf{k}}(\omega)|^2\rangle}\,. \tag{4}$$

With the quasinormal approximation (so that the ensemble average of cross products involving four distinct Fourier modes vanishes), it can be shown by substituting $\tilde{\varphi}^*_{\mathbf{k}}$ from Eq. (3) into Eq. (4) that

$$\gamma^2_{\mathbf{k},\mathbf{k}'}(\omega,\omega')=\frac{2|A_{\mathbf{k},\mathbf{k}'}/(L_{\mathbf{k}}+i\omega)|^2\langle|\tilde{\varphi}_{\mathbf{k}'}(\omega')\tilde{\varphi}_{\mathbf{k}-\mathbf{k}'}(\omega-\omega')|^2\rangle}{\sum_{\omega',\mathbf{k}'}|A_{\mathbf{k},\mathbf{k}'}/(L_{\mathbf{k}}+i\omega)|^2\langle|\tilde{\varphi}_{\mathbf{k}'}(\omega')\tilde{\varphi}_{\mathbf{k}-\mathbf{k}'}(\omega-\omega')|^2\rangle}\,. \tag{5}$$

By summing the squared bicoherence [Eq. (5)] over ω' and $\mathbf{k}'$, we find an important relationship that

$$\sum_{\omega',\mathbf{k}'}\gamma^2_{\mathbf{k},\mathbf{k}'}(\omega,\omega')=1 \tag{6}$$

within the reduced triangular spectral region. (Note that the total squared bicoherence over the full spectral region is 2.) The above result says that the full spectral squared bicoherence $\gamma^2_{\mathbf{k},\mathbf{k}'}(\omega,\omega')$ is a measure of the relative contribution from each of the interacting pairs $\tilde{\varphi}_{\mathbf{k}'}(\omega')$ and $\tilde{\varphi}_{\mathbf{k}-\mathbf{k}'}(\omega-\omega')$. When there are only a few modes involved in the nonlinear interaction, the typical $\gamma^2_{\mathbf{k},\mathbf{k}'}$ would be high. As the number of modes involved in the coupling increases, the average $\gamma^2_{\mathbf{k},\mathbf{k}'}$ reduces owing to the condition imposed by Eq. (6).

In the experiment, the time behavior of $\tilde{\varphi}(t,\mathbf{x})$ is measured only at a few specific positions. With such limited spatial information, it is not possible to resolve the measurement into individual $\mathbf{k}$ modes. Nevertheless, we can compute an autobicoherence from a single point measurement. For homogeneous turbulence, the ensemble average quantities are independent of $\mathbf{x}$ (i.e., poloidal and toroidal positions) and we can relate the autobicoherence, as defined in Eq. (1), in terms of the spectral components to yield

$$\gamma^2(\omega_1,\omega_2)=\frac{|\sum_{\mathbf{k}',\mathbf{k}}[A^*_{\mathbf{k},\mathbf{k}'}/(L^*_{\mathbf{k}}-i\omega)]\langle|\tilde{\varphi}_{\mathbf{k}'}(\omega_1)\tilde{\varphi}_{\mathbf{k}-\mathbf{k}'}(\omega_2)|^2\rangle|^2}{\sum_{\mathbf{k}',\mathbf{k}}\langle|\tilde{\varphi}_{\mathbf{k}'}(\omega_1)\tilde{\varphi}_{\mathbf{k}-\mathbf{k}'}(\omega-\omega')|^2\rangle\sum_{\omega_1+\omega_2=\omega}\sum_{\mathbf{k}',\mathbf{k}}|A_{\mathbf{k},\mathbf{k}'}/(L_{\mathbf{k}}+i\omega)|^2\langle|\tilde{\varphi}_{\mathbf{k}'}(\omega_1)\tilde{\varphi}_{\mathbf{k}-\mathbf{k}'}(\omega_2)|^2\rangle}\,. \tag{7}$$

Applying the Schwartz inequality to the numerator in Eq. (7), we find quite generally that

$$\sum_{\omega_1+\omega_2=\omega} \gamma^2(\omega_1,\omega_2) \leq 1 .$$

It can be seen from an inspection of Eq. (7) that the total squared autobicoherence is reduced by turbulence broadening. In the absence of broadening, i.e., when modes lie on a well-defined dispersion such that $\tilde{\varphi}_{\mathbf{k}}(\omega) = \tilde{\varphi}(\omega)\delta(\mathbf{k}-\bar{\mathbf{k}}(\omega))$, the total squared autobiocoherence is exactly unity. (We note that $\omega = \omega_L + \Delta\omega_{\mathrm{NL}} = \omega_1 + \omega_2$ is the nonlinear mode frequency and $\Delta\omega_{\mathrm{NL}}$ the nonlinear frequency shift; i.e., the well-defined dispersion needs not be the linear dispersion curve as given by $L_{\mathbf{k}} + i\omega = 0$.) In fact, one can show that $\sum \gamma^2(\omega_1,\omega_2) \approx 1 - \delta^2$ where $\delta \sim \nu_B/\omega$ with ν_B the turbulence frequency broadening.

In the edge plasma of tokamak TEXT, quasicoherent peaks are often observed in the power spectra of fluctuation data measured near the major resonant magnetic flux surfaces. These quasicoherent peaks have low frequency and long wavelength (low m) relative to the small-scale broadband activity. In spite of the differences in their linear properties, the quasicoherent mode is nonlinearly coupled to the short-wavelength modes, especially those with frequencies below the broadband peak. This means that the relatively low-m modes should be considered as components of the edge turbulence. When they are included, the localization and q-dependence properties of the turbulence become obvious. These properties imply that radial eigenmode structure is relevant in modeling the edge turbulence. The q-dependence property is also discernible in the behavior of the overall wave number spectral width in some experiments [3,22]. The bispectral analysis of edge fluctuation data further indicates that the nonlinear interactions involving the long-wavelength modes are coherent; a signature of regular or coherent structure. The coherent interactions also imply that the nonlinear process may generate a frequency shift (from the linear mode frequency) but not a substantial frequency broadening. These results suggest that the nonlinear dispersion might be a fairly well defined curve in the plasma frame and that the spectrum observed in experiment (i.e., in the laboratory frame) might be broadened by finite radial resolution in measurement and variations in the plasma rotation.

In summary, we have established that the long-wavelength modes localized to major resonant surfaces are indeed part of the turbulence system and that coherent nonlinear coupling (indicative of regular structure) exists in the vicinity of these low-order resonant surfaces. These studies extend our general knowledge of plasma turbulence. We have identified a path (i.e., nonlinear coupling to the transport-related turbulence) through which the long-wavelength modes can influence transport. If the long-wavelength modes are unstable, they could even provide the sustenance needed to maintain the turbulent system. Further work is needed to determine the direction of energy flow and the exact role of the long-wavelength modes in confinement.

The authors would like to acknowledge useful discussions with W. Horton, B. Carreras, and P. Terry. This work was supported by the U.S. Department of Energy, Office of Fusion Energy, Contract No. DE-FG05-89ER53267.

[a]Permanent address: University of Tromsø, 9000 Tromsø, Norway.

[1] J. D. Callen, B. A. Carreras, and R. D. Stambaugh, Phys. Today **45**, No. 1, 34 (1992).
[2] A. J. Wootton, B. A. Carreras, H. Matsumoto, K. McGuire, W. A. Peebles, Ch. P. Ritz, P. W. Terry, and S. J. Zweben, Phys. Fluids B **2**, 2879 (1990).
[3] H. Y. W. Tsui *et al.*, J. Nucl. Mater. **196-198**, 794 (1992).
[4] J.-N. Leboeuf, D. K. Lee, B. A. Carreras, N. Dominguez, P. H. Diamond, A. S. Ware, Ch. P. Ritz, A. J. Wootton, W. L. Rowan, and R. V. Bravenec, Phys. Fluids B **3**, 2291 (1991).
[5] A. Hasegawa and C. G. Maclennan, Phys. Fluids **22**, 2122 (1979).
[6] J. D. Meiss and W. Horton, Phys. Fluids **26**, 990 (1983).
[7] M. Kono and E. Miyashita, Phys. Fluids **31**, 326 (1988).
[8] A. Muhm, A. M. Pukhov, K. H. Spatschek, and V. Tsytovich, Phys. Fluids B **4**, 336 (1992).
[9] P. W. Terry, D. E. Newman, H. Biglari, R. Nazikian, P. H. Diamond, V. Lebedev, Y. Liang, V. Shapiro, V. Schevchenko, B. A. Carreras, K. Sidikman, L. Garcia, G. G. Craddock, J. Crotinger, and A. E. Koniges, in Plasma Physics and Controlled Nuclear Fusion Research 1992, Proceedings of the Fourteenth International Conference, Würzburg, 1992 (to be published).
[10] Ch. P. Ritz, Roger D. Bengtson, S. J. Levinson, and E. J. Powers, Phys. Fluids **27**, 2925 (1984); C. P. Ritz, D. L. Brower, T. L. Rhodes, R. D. Bengtson, S. J. Levinson, N. C. Luhmann, Jr., W. A. Peebles, and E. J. Powers, Nucl. Fusion **27**, 1125 (1987).
[11] H. Y. W. Tsui, P. M. Schoch, and A. J. Wootton, Phys. Fluids B **5**, 1274 (1993).
[12] J. M. Beall, Y. C. Kim, and E. J. Powers, J. Appl. Phys. **53**, 3933 (1982).
[13] C. S. Chang, R. R. Dominguez, and R. D. Hazeltine, Phys. Fluids **24**, 1655 (1981).
[14] R. D. Hazeltine, D. Doborott, and T. S. Wang, Phys. Fluids **18**, 1778 (1975).
[15] J. F. Drake and Y. C. Lee, Phys. Fluids **20**, 1341 (1977).
[16] N. T. Gladd, J. F. Drake, C. L. Chang, and C. S. Liu, Phys. Fluids **23**, 1182 (1980).
[17] A. B. Hassam and J. F. Drake, Phys. Fluids **26**, 133 (1983).
[18] Y. C. Kim and E. J. Powers, IEEE Trans. Plasma Sci. **7**, 120 (1979).
[19] Ch. P. Ritz, E. J. Powers, and R. D. Bengtson, Phys. Fluids B **1**, 153 (1989).
[20] A. Hasegawa and K. Mima, Phys. Rev. Lett. **39**, 205 (1977).
[21] K. Rypdal, Phys. Scr. **23**, 277 (1981).
[22] Ch. P. Ritz *et al.*, in *Plasma Physics and Controlled Nuclear Fusion Research, 1990* (International Atomic Energy Agency, Vienna, 1991), Vol. 2, p. 589.